Electronic Supplementary Material (ESI) for RSC Advances.

Supporting Information

Synthesis of novel hybrid mesoporous gold iron oxide nanoconstructs for enhanced catalytic reduction and remediation of toxic organic pollutants

Kheireddine El-Boubbou,[abc]* O. M. Lemine,[d] and Daniel Jaque[b]

[a]King Saud bin Abdulaziz University for Health Sciences (KSAU-HS) & King Abdullah International Medical Research Center (KAIMRC), King Abdulaziz Medical City, National Guard Health Affairs, Riyadh 11426, Saudi Arabia

[b]Nanomaterials for Bioimaging Group (nanoBIG), Facultad de Ciencias, Departamento de Física de Materiales, Universidad Autónoma de Madrid (UAM), Madrid 28049, Spain

[c]Department of Chemistry, College of Science, University of Bahrain, Sakhir 32038, Kingdom of Bahrain

[d]Department of Physics, College of Sciences, Imam Mohammad Ibn Saud Islamic University (IMSIU), Riyadh 11623, Saudi Arabia

Correspondence* E-mail: elboubboukh@ngha.med.sa

TEM

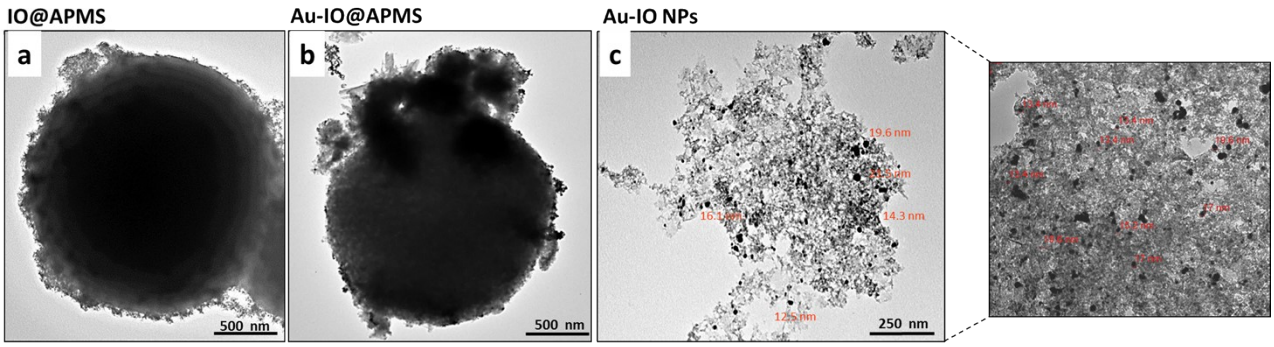

Figure S1. TEM images of the mesoporous Au-IO samples: a) IO@APMS-Amine, b) Au-grafted IO@APMS, and c) Au-IO NPs. The images clearly shows the grafting of AuNPs (15-20 nm) onto IO@APMS-Amine and the successful etching to afford Au-IO mesostructures.

EDX Elemental Analysis

Au-IO@APMS

Element	Weight %	Atomic %
O	43.7	72.0
Si	11.7	11.1
Fe	32.1	15.2
Au	12.5	1.7

Au-IO NPs

Element	Weight %	Atomic %
O	36.6	70.6
Si	0.5	0.5
Fe	48.3	26.6
Au	14.6	2.3

Table S1. EDX elemental analysis of the Au-incorporated IO samples selected from their respective SEM images.

DLS and Zeta Potential

IO@APMS-Amine & Au-IO@APMS

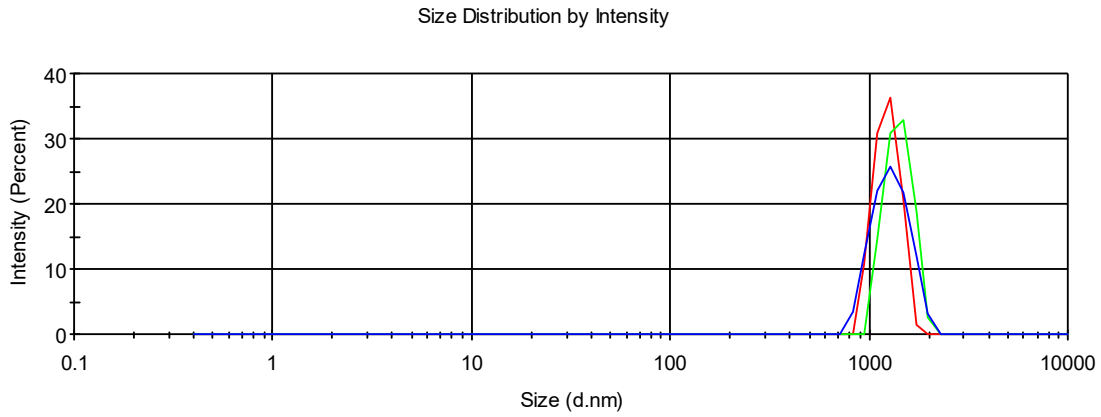

Mesoporous Au-IO NPs

Figure S2. A) DLS measurements of the three different mesoporous IO@APMS-Amine, Au-IO@APMS, and Au-IO samples dispersed in aqueous media. IO@APMS-Amine (D_H = 1475 ± 117 nm), Au-IO@APMS (D_H = 1565 ± 182 nm), and Au-IO mesostructures ((D_H = 710 ± 55 nm). Three independent measurements for three different concentrations were conducted reported as average means ± Std. Dev.

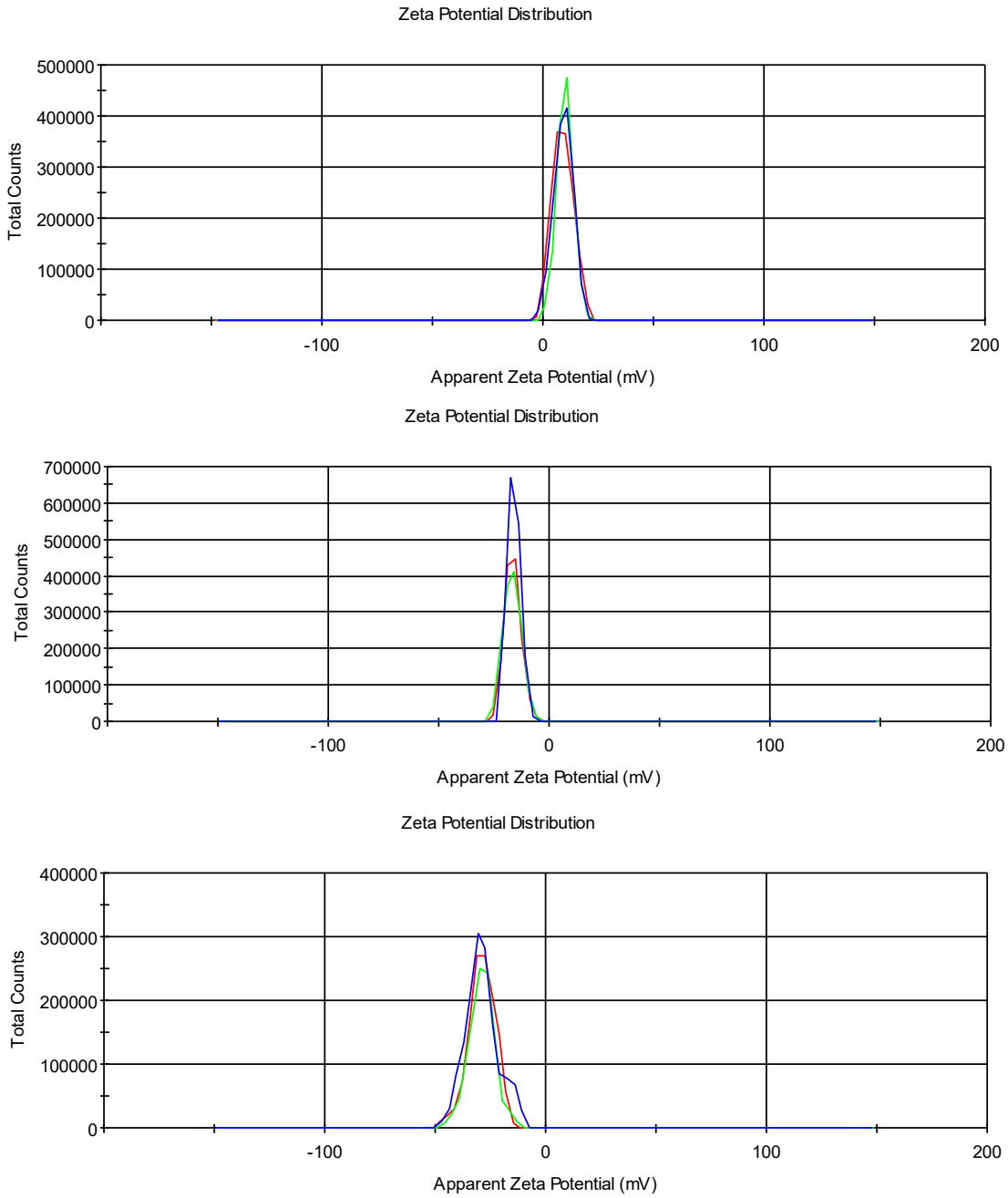

Figure S2. B) Zeta potential (ξ) measurements of IO@APMS-Amine (ξ = +9.40 ± 0.56 mV), Au-IO@APMS (ξ = –16.8 ± 0.50 mV), and Au-IO mesostructures (–26.4 ± 0.98 mV). Three independent measurements for three different concentrations were conducted reported as average means ± Std. Dev.

Magnetic Properties

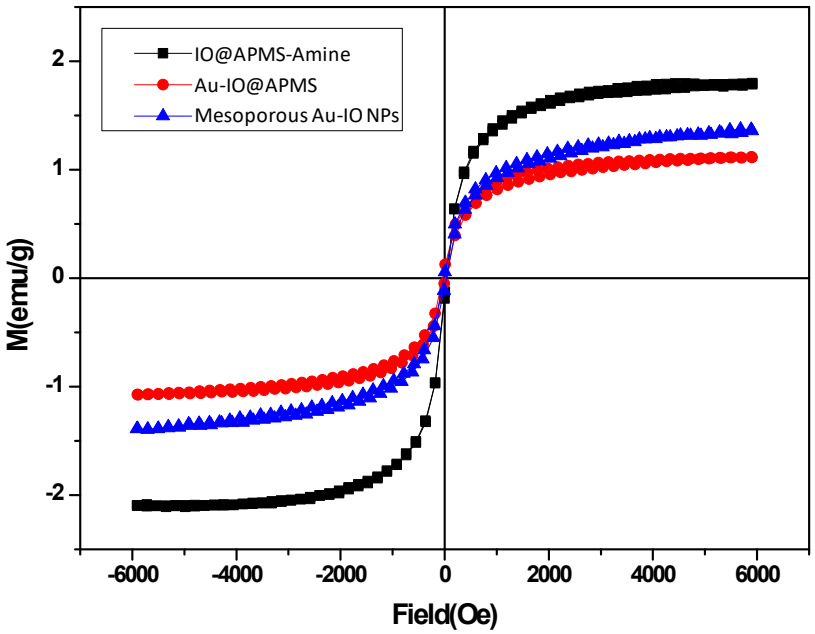

Figure S3. Field-dependent magnetization (*M-H*) hysteresis loops for the three different mesoporous samples clearly showing their superparamagnetic nature (M_s of IO@APMS-Amine = 1.85 emu/g, Au-IO@APMS = 1.09 emu/g, and mesoporous Au-IO = 1.36 emu/g).

XRD

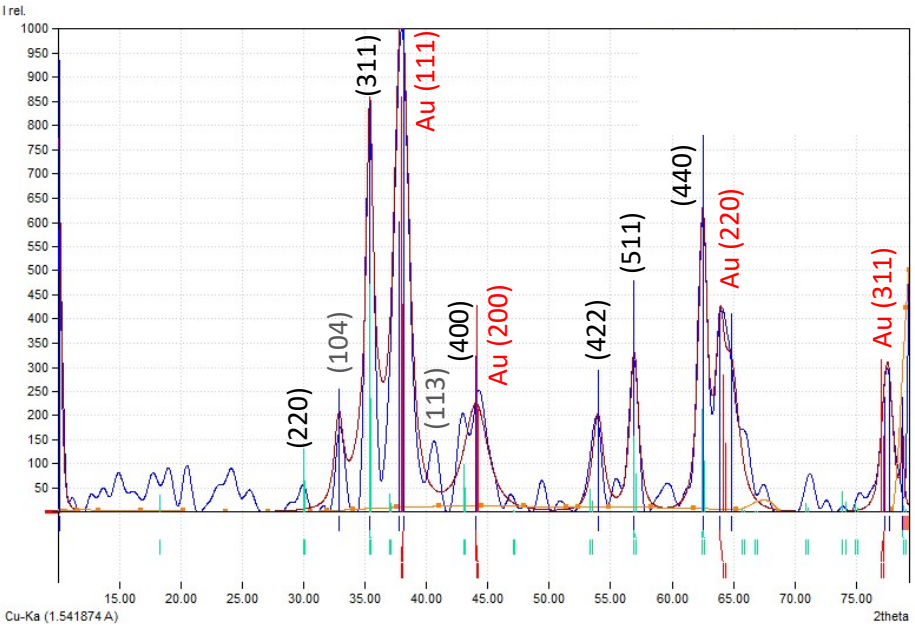

Figure S4. X-ray diffraction patterns showing γ-Fe_2O_3 maghemite (black) and Au phases (red).

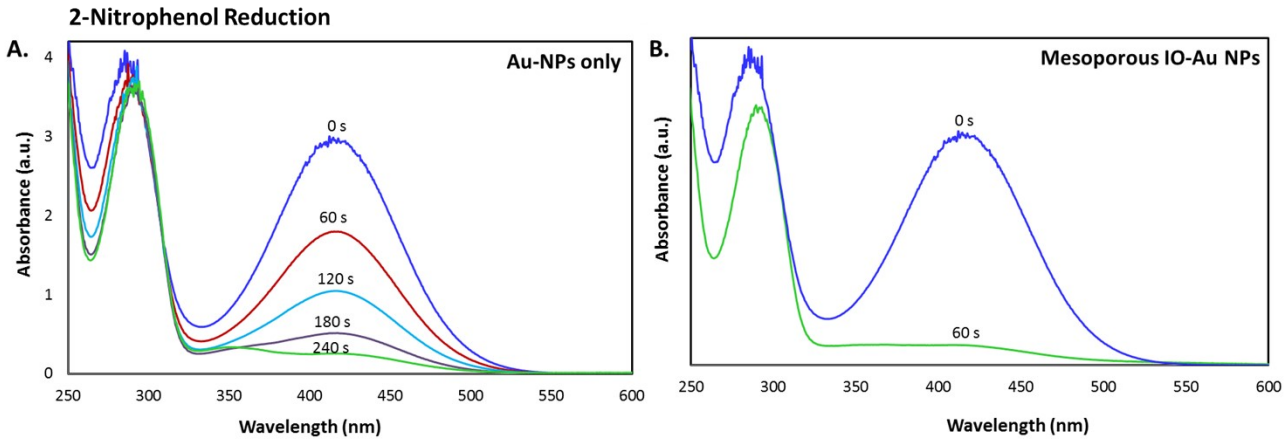

Figure S5. Time progressive UV-vis absorption spectra of 2-nitrophenol reduction using same concentrations of Au-NPs only and mesoporous IO-Au NPs. Reaction conditions: 2.5 mM of nitrophenol solution, 25 mM of freshly prepared $NaBH_4$ (excess), 1.5 mg of catalyst, total volume = 1 mL.

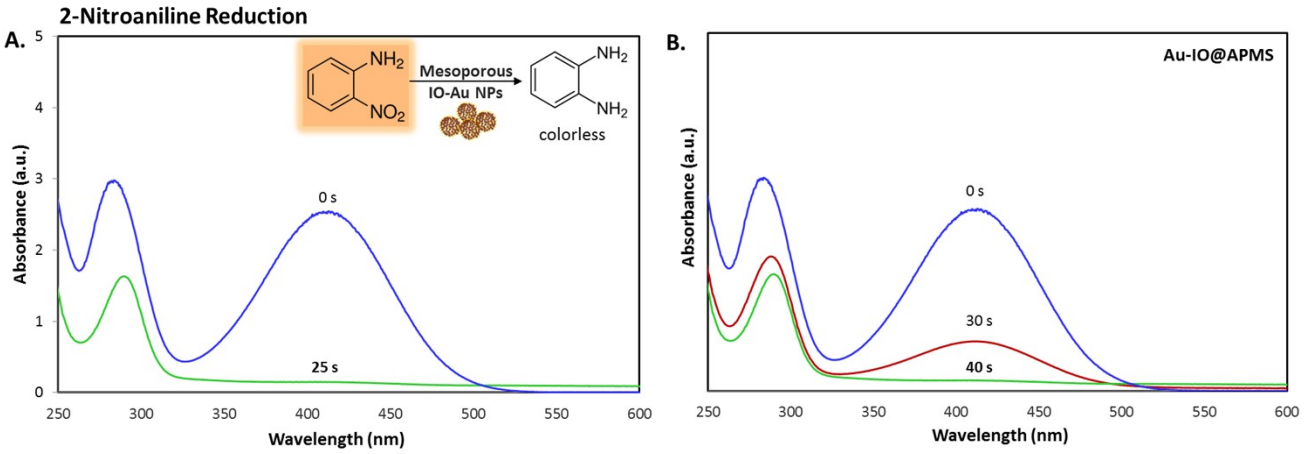

Figure S6. Time progressive UV-vis absorption spectra of 2-nitroaniline reduction using mesoporous nanocatalysts a) IO-Au NP and b) Au-IO@APMS. Reaction conditions: 2.5 mM of nitroaniline solution, 25 mM of freshly prepared $NaBH_4$ (excess), 1.5 mg of catalyst, total volume = 1 mL.